Available online at www.sciencedirect.com
SCIENCE DIRECT®
Journal of Sound and Vibration 277 (2004) 133–148
JOURNAL OF SOUND AND VIBRATION
www.elsevier.com/locate/jsvi

A model of the correlation function of leak noise in buried plastic pipes

Y. Gao[a,*], M.J. Brennan[a], P.F. Joseph[a], J.M. Muggleton[a], O. Hunaidi[b]

[a] *Institute of Sound and Vibration Research, University of Southampton, Southampton SO17 1BJ, UK*
[b] *National Research Council of Canada, Institute for Research in Construction, Ottawa, Canada K1A 0R6*

Received 25 February 2003; accepted 26 August 2003

Abstract

A common technique for locating leaks in buried water distribution pipes is the use of the cross-correlation on two measured acoustic signals, on either side of a leak. This technique can be problematic for locating leaks in plastic pipes as the acoustic signals in these pipes are generally narrow-band and low frequency. The effectiveness of the cross-correlation technique for detecting leaks in plastic pipes has been investigated experimentally in an earlier study. This paper develops an analytical model to predict the cross-correlation function of leak signals in plastic pipes. The model is based on a theoretical formulation of wave propagation in a fluid-filled pipe in vacuo and the assumption that the leak sound, at source, has a flat spectrum over the bandwidth of interest. The analytical model is used to explain some of the features of correlation measurements made in actual water pipes. Leak noise signals are generally passed through a band-pass filter before calculating the cross-correlation function. The model is used to demonstrate the importance of the cut-off frequency of the high-pass filter and the insensitivity of the correlation to the cut-off frequency of the low-pass filter.

1. Introduction

Water leakage from buried pipes is a subject of increasing concern because of decreasing water supplies due to changing rainfall patterns, deterioration or damage to the distribution system, and ever increasing water demand. A leak from a water supply pipe generates noise, which can be used for leak detection and location. Acoustic leak detection techniques have been shown to be effective [1–3] and are in common use in the water industry. Other methods of leak detection which have been used with varying degrees of success, are tracer gas, thermography [4], flow and

*Corresponding author. Tel.: +44-23-8059-3756; fax: +44-23-8059 3190.
E-mail address: gy@isvr.soton.ac.uk (Y. Gao).

0022-460X/$ - see front matter
doi:10.1016/j.jsv.2003.08.045

pressure modelling [5], and ground penetrating radar (GPR) [6]. The potential of several non-acoustic technologies has been evaluated by Hunaidi et al. [7,8]. Although they show some promise, these non-acoustic techniques are more complex and time-consuming, and may fail to detect leaks in practical situations.

In leak detection surveys using acoustic signals, the most widely used technique for locating leaks is the correlation technique. Recent work on typical PVC water distribution pipes has focused on the dominant low frequency signals [8,9], since the acoustic signals in plastic pipes are heavily attenuated and generally narrow-band and of low frequency. The effectiveness of the correlation technique was found to be affected by several factors, including the selection of vibration sensors and cut-off frequencies of high and low-pass digital filters used to remove noise in the frequency range in which the signal is weak. Although it has been shown that leaks in plastic pipes can be located using the correlation technique, the effect of the filter cut-off frequencies has only been studied empirically.

This paper develops an analytical model of the cross-correlation function, which is then used to investigate the effect of band-pass filtering on leak detection in buried plastic water pipes. Since the effectiveness of the correlation technique is largely influenced by background noise, the effect of the background noise on the model is also discussed. The model is also used to explain the features of some experimental data, and to demonstrate the importance of the cut-off frequency of the high-pass filter.

2. Leak detection using correlation

The cross-correlation technique is straightforward. Vibration or acoustic signals are measured using either accelerometers or hydrophones at two access points, on either side of the location of a suspected leak. The signals from the sensors are transmitted to the leak noise correlator, which computes the cross-correlation function of the two signals and presents the results to an operator. Fig. 1 depicts a typical measurement arrangement for a water leak in a buried water pipe, and access points (normally a fire hydrant) where a sensor can be attached is located on each side of the leak at distances d_1 and d_2. In the analysis presented in this paper the pipe is assumed to be of

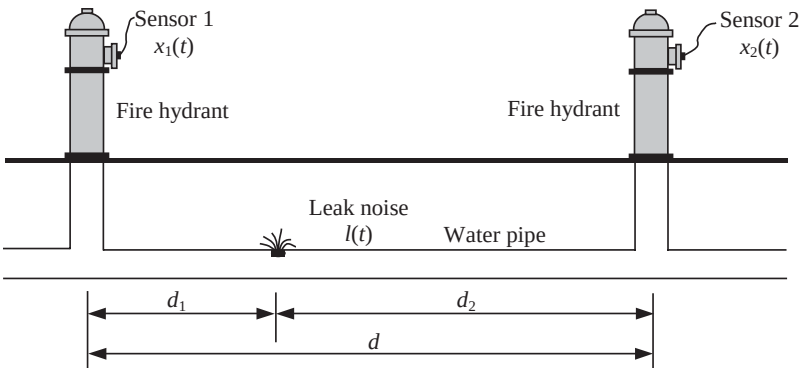

Fig. 1. Schematic of a pipe with a leak bracketed by two sensors.

infinite length, without reflecting discontinuities for the predominantly fluid-borne wave, at all frequencies of interest.

Consider the situation where the data measured are two continuous random signals $x_1(t)$ and $x_2(t)$, which are assumed to be stationary (ergodic). Setting the mean value of each signal to zero, the cross-correlation function is defined by [10]

$$R_{x_1x_2}(\tau) = E[x_1(t)x_2(t+\tau)], \tag{1}$$

where τ is the lag of time; $E[\,]$ is the expectation operator. The argument τ that maximizes Eq. (1) provides an estimate of the time delay τ_{peak}. In practice, however, $R_{x_1x_2}(\tau)$ can only be estimated as signals are always measured during a finite time interval. For example, if the two signals $x_1(t)$ and $x_2(t)$ are measured in a common time interval $0 \leqslant t \leqslant T$, the biased correlation estimator, $\hat{R}_{x_1x_2}(\tau)$, is given by [10]

$$\hat{R}_{x_1x_2}(\tau) = \frac{1}{T}\int_0^{T-\tau} x_1(t)x_2(t+\tau)\,\mathrm{d}t, \quad \tau > 0,$$
$$\hat{R}_{x_1x_2}(\tau) = \frac{1}{T}\int_{-\tau}^{T} x_1(t)x_2(t+\tau)\,\mathrm{d}t, \quad \tau < 0. \tag{2}$$

A procedure for the implementation of the cross-correlation function using sampled data is illustrated in Fig. 2, where $*$ denotes conjugation. The required correlation estimator can be derived from the inverse Fourier transform of $X_1^*(f)X_2(f)$ and scaled appropriately for normalization, where $X_1(f)$ and $X_2(f)$ are the Fourier transforms of $x_1(t)$ and $x_2(t)$, respectively.

It is useful to express the cross-correlation function in a normalized form, which has a scale of -1 to $+1$, namely the correlation coefficient $\rho_{x_1x_2}(\tau)$ defined as

$$\rho_{x_1x_2}(\tau) = \frac{R_{x_1x_2}(\tau)}{\sqrt{R_{x_1x_1}(0)R_{x_2x_2}(0)}}, \tag{3}$$

where $R_{x_1x_1}(0)$ and $R_{x_2x_2}(0)$ are the values of auto-correlation functions $R_{x_1x_1}(\tau)$ and $R_{x_2x_2}(\tau)$ at $\tau = 0$.

If a leak exists between the two sensor positions, a distinct peak may be found in the cross-correlation function. This gives the time delay τ_{peak} that corresponds to the difference in arrival times between the signals at each sensor. The location of the leak relative to one of the measurement points is easily calculated using a simple algebraic relationship between the time delay, the distance d between the access points and the propagation wavespeed c in the buried

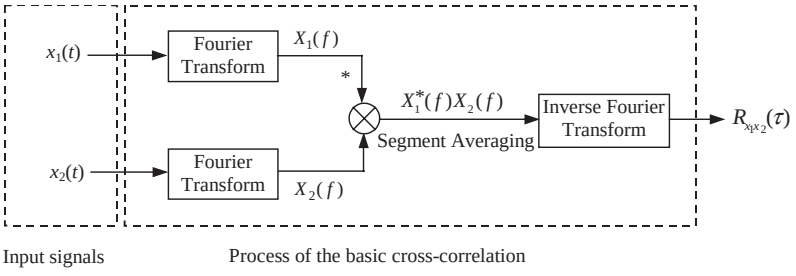

Fig. 2. Schematic of the implementation of the basic cross-correlation function.

pipe. With reference to Fig. 1, the time delay is related to the locations of the sensors by

$$\tau_{peak} = \frac{d_2 - d_1}{c}. \tag{4}$$

By substituting $d_2 = d - d_1$ into Eq. (4), the position of the leak relative to sensor 1 is found to be

$$d_1 = \frac{d - c\tau_{peak}}{2}. \tag{5}$$

3. Wave propagation in plastic pipes

The theory of vibration and wave propagation in thin-walled shells in vacuo and in fluid-filled pipes has been summarized by Fuller and Fahy [11,12] and Pinnington and Briscoe [13]. Experimental work has been carried out by Muggleton et al. [14] to validate the analytical predictions of axisymmetric wavespeed and attenuation for a fluid-filled elastic pipe in vacuo. More recently Muggleton et al. [15] have investigated the effects of the ground on wave propagation in buried pipes. They found that the effect of the surrounding medium is to mass load the pipe, but at low frequencies its effect on the speed of the propagating wave is relatively small compared with a fluid-filled pipe in vacuo. Therefore, the analytical model for a fluid-filled pipe in vacuo developed by Pinnington and Briscoe [13] is used in this paper. At low frequencies, well below the pipe ring frequency, the predominantly fluid-borne wave, which is responsible for the propagation of leak noise, has a wavenumber k given by

$$k^2 = k_f^2\left(1 + \frac{2Ba}{Eh + \mathrm{i}\eta Eh}\right), \tag{6}$$

where k_f is the free-field fluid wavenumber and η is the loss factor of the pipe wall; a, h are the pipe radius and wall thickness; E is Young's modulus of pipe wall material; and B is the fluid bulk modulus of elasticity.

In the frequency range where the wavelength of the predominantly fluid-borne wave is much greater than the diameter of the pipe (which is the case considered in this paper), the acoustic pressure can be considered to be uniform across the cross-section, and is given by [13,14]

$$p(x) = P_0(\omega)\mathrm{e}^{-\mathrm{i}kx}, \tag{7}$$

where x is the distance between the leak and sensor signals; $P_0(\omega)$ is the amplitude of the acoustic pressure at $x = 0$ and k is the complex fluid-borne wavenumber given by Eq. (6), the real part of which gives the wavespeed, which can be represented as

$$\mathrm{Re}\{k\} = \frac{\omega}{c}, \tag{8}$$

where c is the wavespeed given by

$$c = c_f\left(1 + \frac{2Ba}{Eh}\right)^{-1/2}, \tag{9}$$

and the imaginary part of which gives the wave attenuation

$$\mathrm{Im}\{k\} = -\beta\omega, \tag{10}$$

where β is a measure of the loss within the pipe wall and is given by

$$\beta = \frac{1}{c_f}\frac{\eta Ba/Eh}{\left(1+(2Ba/Eh)\right)^{1/2}}, \tag{11}$$

where c_f is the fluid wavespeed. Eq. (9) indicates that the propagation wavespeed is independent of frequency at low frequencies. The attenuation (loss) of the amplitude of the propagating wave in dB/m is given by

$$Attenuation = -\frac{20\mathrm{Im}\{k\}}{\ln(10)} = 8.67\beta\omega. \tag{12}$$

For a typical PVC pipe with $a/h = 10$, $E = 5\times10^9\,\mathrm{N/m^2}$, $\mathrm{Re}\{k\}\approx 3.2k_f$. For an even softer pipe wall, the wavenumber, k, is much greater than the wavenumber in the infinite medium. This indicates that the wavespeed of the fluid-borne wave for the plastic pipe decreases rapidly with increasing fluid loading (decreasing pipe wall stiffness). Eq. (12) shows that wave attenuation in fluid-filled plastic pipes increases with frequency.

4. Combining the correlation technique with the wave propagation model

From Eq. (7), the frequency response function between the leak and the sensor signal is given by

$$H(\omega, x) = \mathrm{e}^{-\mathrm{i}\omega x/c}\mathrm{e}^{-\omega\beta x}. \tag{13}$$

For two signals $x_1(t)$ and $x_2(t)$ measured at positions $x = d_1$ and $x = d_2$, the cross-spectral density $S_{x_1x_2}(\omega)$ can be obtained by

$$S_{x_1x_2}(\omega) = \frac{1}{2\pi}\lim_{T\to\infty} E\left[\frac{X_{1T}^*(\omega)X_{2T}(\omega)}{T}\right] = S_{ll}(\omega)\Psi(\omega)\,\mathrm{e}^{\mathrm{i}\omega T_0}, \tag{14}$$

where $S_{ll}(\omega)$ is the auto-spectral density of the leak signal $l(t)$, which is the acoustic pressure at the leak location; T_0 is the time shift given by $T_0 = -(d_2 - d_1)/c$; and $\Psi(\omega) = \left|H_1^*(\omega, x_1)H_2(\omega, x_2)\right| = \mathrm{e}^{-\omega\beta(d_2+d_1)}$. The phase spectrum between the two signals is related to the time shift that the signals experience as they propagate through the pipe, which is given by

$$\Phi_{x_1x_2}(\omega) = \mathrm{Arg}\{S_{x_1x_2}(\omega)\} = \omega T_0. \tag{15}$$

Since multiplication in one domain corresponds to convolution in the transformed domain, the cross-correlation function $R_{x_1x_2}(\tau)$ is determined by

$$R_{x_1x_2}(\tau) = F^{-1}\{S_{x_1x_2}(\omega)\} = R_{ll}(\tau)\otimes\psi(\tau)\otimes\delta(\tau + T_0), \tag{16}$$

where $F^{-1}\{\,\}$ denotes the inverse Fourier transform; $\otimes$ denotes convolution; the auto-correlation of the leak signal $R_{ll}(\tau) = F^{-1}\{S_{ll}(\omega)\}$; $\psi(\tau)$ is given by

$$\psi(\tau) = F^{-1}\{\Psi(\omega)\} = \frac{\beta d}{\pi[(\beta d)^2 + \tau^2]}, \tag{17}$$

and $\delta(\tau)$ is the Dirac delta function. An interpretation of Eq. (16) is that the delta function $\delta(\tau + T_0)$ is broadened by the introduction of the band-limited leak spectrum $S_{ll}(\omega)$ and the nature of $\Psi(\omega)$. The spectral characteristics of the leak noise are not currently known, but for the purpose of the analysis in this paper a flat leak spectrum is assumed. Under the assumption that $S_{ll}(\omega)$ is a constant S_0, Eq. (16) shows that the cross-correlation function only depends upon the frequency attenuation of the plastic pipe and the distance between the sensors.

Thus it is more difficult to estimate the time delay from the correlation function if the pipe is heavily damped and/or the measurement positions where the sensor attached are far from the source of the leak.

For most plastic pipework systems, leak detection is successful with low frequency leak signals resulting from a non-dispersive propagating wave with a constant attenuation factor β. In practice, band-pass filtering operations are performed to attenuate the signals outside the frequency range of interest. For the simple case where an ideal band-pass filter is applied to remove the noise, the frequency behaviour of the filter is described by

$$\begin{aligned} G(\omega) &= 1 \quad \omega_0 \leqslant |\omega| < \omega_1; \\ &= 0 \qquad \text{otherwise.} \end{aligned} \tag{18}$$

Assuming that $S_{ll}(\omega) = S_0$ in the frequency range ω_0 to ω_1, the cross-correlation function of Eq. (16) becomes

$$R_{x_1x_2}(\tau) = S_0\psi(\tau) \otimes g(\tau) \otimes \delta(\tau + T_0), \tag{19}$$

where

$$g(\tau) = F^{-1}\{G(\omega)\} = \frac{\Delta\omega}{\pi}\frac{\sin(\Delta\omega\tau/2)\cos(\omega_c\tau)}{\Delta\omega\tau/2},$$

and $\Delta\omega = \omega_1 - \omega_0$ is the bandwidth of the band-pass filter. Eq. (19) can be written as

$$R_{x_1x_2}(\tau) = \frac{S_0 e^{-\omega_0\beta d}}{\pi\sqrt{(\beta d)^2 + (\tau + T_0)^2}}[\cos(\omega_0(\tau + T_0) + \theta) - e^{-\Delta\omega\beta d}\cos(\omega_1(\tau + T_0) + \theta)], \tag{20}$$

where $\theta = \tan^{-1}(\tau/\beta d)$. If the frequency bandwidth satisfies the condition $e^{-\Delta\omega\beta d} \ll 1$, Eq. (20) can be approximated by

$$R_{x_1x_2}(\tau) \approx \frac{S_0 e^{-\omega_0\beta d}}{\pi\sqrt{(\beta d)^2 + (\tau + T_0)^2}}\cos(\omega_0\tau + \theta). \tag{21}$$

Compared with Eq. (20), the interference term caused by the upper cut-off frequency ω_1 does not appear in Eq. (21). Therefore, provided that the bandwidth of the filter is relatively broad, the cross-correlation function is mainly dominated by the lower cut-off frequency ω_0. This is because the pipe effectively acts as a low-pass filter, because of damping in the pipe-wall as shown in Eq. (13).

Following a similar analysis to the cross-correlation function, the auto-correlation $R_{xx}(\tau)$ is found to be

$$R_{xx}(\tau) = S_0\varphi(\tau) \otimes g(\tau), \tag{22}$$

where

$$\varphi(\tau) = F^{-1}\{|H(\omega, x)|^2\} = \frac{2\beta x}{\pi\sqrt{(2\beta x)^2 + \tau^2}}.$$

Eq. (22) can also be written as

$$R_{xx}(\tau) = \frac{S_0 e^{-2\omega_0\beta x}}{\pi\sqrt{(2\beta x)^2 + \tau^2}}[\cos(\omega_0\tau + \theta) - e^{-2\Delta\omega\beta x}\cos(\omega_1\tau + \theta)]. \tag{23}$$

Substituting Eqs. (20) and (23) into Eq. (3) gives the cross-correlation coefficient as

$$\rho_{x_1x_2}(\tau) = \frac{2\beta\sqrt{d_1 d_2}}{\sqrt{(\beta d)^2 + (\tau + T_0)^2}} \frac{\cos(\omega_0(\tau + T_0) + \theta) - e^{-\Delta\omega\beta d}\cos(\omega_1(\tau + T_0) + \theta)}{(1 - e^{-2\Delta\omega\beta d_1})^{1/2}(1 - e^{-2\Delta\omega\beta d_2})^{1/2}}. \tag{24}$$

At $\tau_{peak} = -T_0 = (d_2 - d_1)/c$, the peak value of the cross-correlation coefficient is

$$\rho_{x_1x_2}(\tau_{peak}) = \frac{2\sqrt{d_1 d_2}}{d} \frac{1 - e^{-\Delta\omega\beta d}}{(1 - e^{-2\Delta\omega\beta d_1})^{1/2}(1 - e^{-2\Delta\omega\beta d_2})^{1/2}}. \tag{25}$$

With reference to Eq. (25), consider the following three cases:

(i) The first case is where both sensors are some distance from the leak and there is no band-pass filter, i.e., $d_1 \approx d_2 \neq 0$, and the frequency bandwidth satisfies $e^{-2\Delta\omega\beta d_1} \ll 1$ (or $e^{-2\Delta\omega\beta d_2} \ll 1$). Eq. (25) then reduces to

$$\rho_{x_1x_2}(\tau_{peak}) = \frac{2\sqrt{d_1 d_2}}{d}. \tag{26a}$$

(ii) The second case is where one sensor is very close to the leak and the other sensor is some distance from the leak, i.e., d_1 is very small such that $d \approx d_2$, and assuming $\Delta\omega$ is still sufficiently large so that $e^{-2\Delta\omega\beta d_2} \ll 1$, but $1 - e^{-2\Delta\omega\beta d_1} \approx 2\Delta\omega\beta d_1$. The peak cross-correlation coefficient given by Eq. (25) then becomes

$$\rho_{x_1x_2}(\tau_{peak}) = \sqrt{\frac{2}{\beta d_2 \Delta\omega}}. \tag{26b}$$

(iii) The third case is when sensors 1 and 2 are interchanged. If d_2 is very small, the peak cross-correlation coefficient is given by

$$\rho_{x_1x_2}(\tau_{peak}) = \sqrt{\frac{2}{\beta d_1 \Delta\omega}}. \tag{26c}$$

A comparison of the peak cross-correlation coefficient given by Eq. (25) and its approximation by Eq. (26a) is shown in Fig. 3. As the product $\Delta\omega\beta d$ increases, the approximation given in

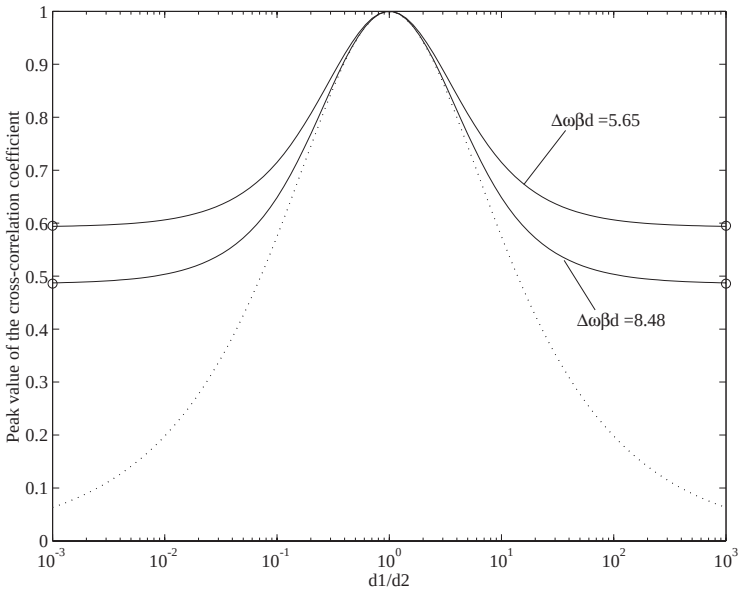

Fig. 3. Peak value of the cross-correlation coefficient as a function of the ratio of the distances d_1 and d_2: ——, theoretical values; · · · ·, approximation.

Eq. (26a) approaches the solution given in Eq. (25). The two points marked by 'o' are given by Eqs. (26b) and (26c), which provide the approximate peak value of the cross-correlation coefficient as one sensor is moved close to the leak. For two equispaced sensors $d_1/d_2 = 1$, the peak cross-correlation coefficient is found to be unity, which simply means that there is a perfect linear relationship between these two sensor signals. For other configurations, good levels of correlation (e.g., greater than about 0.5) are only possible for ratios of sensor distances from the leak of less than about 10 (or greater than 0.1). In practical situations, background noise also has an effect on the correlation. In Section 6 the theoretical predictions are compared with experimental data, which, inevitably, will be contaminated by noise. To make this comparison, therefore, the effect of noise on the peak correlation needs to be included in the model, and this is discussed in the next section.

5. Effect of the background noise on the correlation technique

The aim of this section is to quantify the effect of noise on the correlation technique, in which noise can be included into the analytical model of the correlation coefficient derived in Section 4. Assume that the leak signals measured by two acoustic sensors are in the presence of the background noise. This can be modelled as

$$x_1(t) = s_1(t) + n_1(t), \tag{27a}$$

and

$$x_2(t) = s_2(t) + n_2(t), \tag{27b}$$

where random processes $s_1(t)$, $s_2(t)$, $n_1(t)$ and $n_2(t)$ are stationary. If the noise at each sensor is assumed to be uncorrelated with each other and with the signals, then the cross-correlation function of signals $x_1(t)$ and $x_2(t)$ is given by

$$R_{x_1x_2}(\tau) = R_{s_1s_2}(\tau). \tag{28}$$

Eq. (28) indicates that effect of the uncorrelated background noise can be removed when correlating the two sensor signals. Noting that $R_{xx}(0) = \sigma_x^2$, the cross-correlation coefficient $\rho_{x_1x_2}(\tau)$ including the effects of noise is given by

$$\rho_{x_1x_2}(\tau) = \frac{R_{x_1x_2}(\tau)}{\sqrt{R_{x_1x_1}(0)R_{x_2x_2}(0)}} = \frac{\rho_{s_1s_2}(\tau)}{\sqrt{\left(1+\dfrac{\sigma_{n_1}^2}{\sigma_{s_1}^2}\right)\left(1+\dfrac{\sigma_{n_2}^2}{\sigma_{s_2}^2}\right)}}, \tag{29}$$

where $\sigma_{s_1}^2$, $\sigma_{s_2}^2$, $\sigma_{n_1}^2$, and $\sigma_{n_2}^2$ are the variances of signals $s_1(t)$, $s_2(t)$ and background noise signals $n_1(t)$, $n_2(t)$, respectively; $\rho_{s_1s_2}(\tau)$ is the theoretical prediction of the cross-correlation coefficient. Eq. (29) shows that the correlation coefficient is strongly affected by the signal to noise ratios at the two measurement positions. Based on information of the acoustical characteristics of the leak signal and the measurement positions, estimates of the signal-to-noise ratios (SNR) for sensor signals can thus be obtained from the correlation coefficient.

In the presence of the background noise, for example at sensor 1, the SNR in terms of the ratio $\sigma_{n_1}^2/\sigma_{s_1}^2$ in Eq. (29) is defined as

$$SNR = 10\log_{10}\left(\frac{\sigma_{s_1}^2}{\sigma_{n_1}^2}\right). \tag{30}$$

Using Eq. (23), the ratio $\sigma_{s_1}^2/\sigma_{s_2}^2$ can be obtained

$$\frac{\sigma_{s_1}^2}{\sigma_{s_2}^2} = \frac{d_2}{d_1}\frac{e^{-2\omega_0\beta d_1}(1-e^{-2\Delta\omega\beta d_1})}{e^{-2\omega_0\beta d_2}(1-e^{-2\Delta\omega\beta d_2})}. \tag{31}$$

Assuming that the noise levels at the two measurement positions are the same, i.e., $\sigma_{n_1}^2 = \sigma_{n_2}^2$, Eq. (31) gives

$$\left[\frac{\rho_{s_1s_2}(\tau)}{\rho_{x_1x_2}(\tau)}\right]^2 = 1 + \left(1+\frac{\sigma_{s_1}^2}{\sigma_{s_2}^2}\right)\frac{\sigma_{n_1}^2}{\sigma_{s_1}^2} + \frac{\sigma_{s_1}^2}{\sigma_{s_2}^2}\left(\frac{\sigma_{n_1}^2}{\sigma_{s_1}^2}\right)^2. \tag{32}$$

Using the ratio of the peak cross-correlation coefficients $\rho_{s_1s_2}(\tau_{peak})/\rho_{x_1x_2}(\tau_{peak})$, the ratio $\sigma_{n_1}^2/\sigma_{s_1}^2$ can be determined from the quadratic Eq. (32). This is then substituted into Eq. (30) to give an estimate of the SNR at sensor 1. A similar procedure can be adopted to obtain the SNR at sensor 2. Noting that the correlation technique is affected by the selection of the cut-off frequencies of high and low-pass digital filters, the SNR can thus be enhanced using carefully selected frequency information.

6. Comparison of predictions with test data

Tests were carried out at a leak detection facility at an experimental site located at a National Research Council site in Canada. The description of the test site and measurement procedures are detailed in Ref. [8]. The signals generated by a joint leak were measured by hydrophones attached to two fire hydrants. Referring to Fig. 1, the distance d between the two sensor signals was 102.6 m, and the distance d_1 from the leak to sensor 1 was 73.5 m. The signals were each passed through an anti-aliasing filter with the cut-off frequency set at 200 Hz. Hydrophone-measured signals of 66-s duration were then digitized at a sampling frequency of 500 samples/s.

6.1. *Validation of theoretical predictions of wavespeed and attenuation for the fluid-borne axisymmetric wave*

Spectral analysis was performed on the digitized data using a 1024-point FFT, and a Hanning window with 40% overlap and power spectrum averaging. The following observations are based on the auto-spectra and coherence functions of the hydrophone-measured signals as plotted in Figs. 4(a)–(c) [8]:

(1) Below 5 Hz the signals were dominated by ambient noise, which most probably corresponds to the longitudinal resonances of the test pipe.
(2) Most of the frequency content of sensor signals was concentrated below 50 Hz.

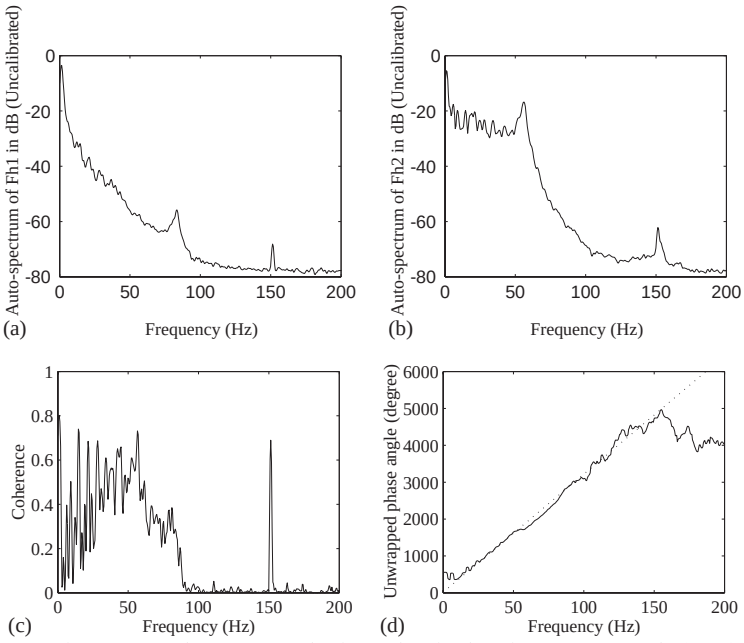

Fig. 4. The auto-spectra, coherence and unwrapped phase for hydrophone-measured signals: (a) auto-spectrum of sensor signal 1; (b) auto-spectrum of sensor signal 2; (c) coherence function; (d) unwrapped phase angle: ——, data measured; · · · ·, Least-squares fit.

(3) Additional peaks in the auto-spectra of the two sensor signals were found at different frequencies, as a result of several factors, including longitudinal resonances of the water pipe, soil resonance, or fundamental frequencies of rotating machinery on the test site, etc.

The fluid-borne axisymmetric wavespeed can be determined from either the frequency response function between two sensor signals or the corresponding cross-spectral density. The same information about the relative phase angle between two sensor signals is provided by these two quantities, which can be seen from Eqs. (13) and (14). The unwrapped phase angle obtained from the hydrophone-measured signals is shown in Fig. 4(d). A straight line indicates that the wavespeed is independent of frequency from 10 to 150 Hz. However, it does not pass through the origin. This is possibly because of the dominant ambient noise at low frequencies. Based on the slope of the least-squares fit line, the wavespeed was calculated to be 479 m/s. There is a good agreement between this value and the results obtained in previous work [9]. This demonstrates that the analytical model is a reasonable representation of the experimental set-up.

The wave attenuation can be derived from the amplitude of the frequency response function between the two sensor signals. Combining Eqs. (10), (12) and (13), gives the rate of attenuation in dB/m as

$$Attenuation = \frac{-20\ln|H(\omega, 1)|}{\Delta d \ln(10)}, \tag{33}$$

where $|H(\omega, x)|$ denotes the amplitude of the frequency response function between the two sensor signals; here x is the distance between the two sensor signals; and the distance difference $\Delta d = d_2 - d_1$. Fig. 5 illustrates the loss in dB/m as a function of frequency based on Eq. (33). The least square fit line gives the attenuation factor β of 2.26×10^{-4} s/m. The rate of attenuation derived

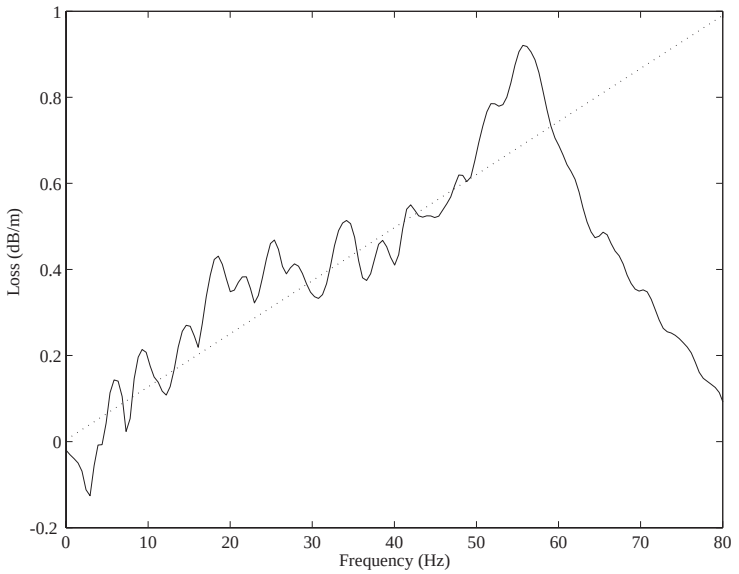

Fig. 5. Loss in dB/m. ——, data measured; · · · ·, least-squares fit.

from hydrophone-measured data confirms that the loss within the pipe increases with increasing frequencies in the frequency range 0–50 Hz.

6.2. Analysis of sensor signals using cross-correlation

As described previously, filtering operations were performed on the digitized sensor signals before conducting the time domain cross-correlation. The sensor signals were then passed through high and low-pass fourth order Butterworth filters. The cross-correlation coefficients were computed using segment averaging via a 1024-point FFT. Meanwhile, the circular effect of the FFT was minimized by 50% zero padding in each segment record. To compare the experimental results with the corresponding theoretical predictions, the effect of the background noise on the theoretical predictions was taken into account by setting the peak values of the cross-correlation coefficients to be the same as those of the experimental results. This enables an estimate of the SNR at the two sensors using the technique outlined in Section 5. When the lower and upper cut-off frequencies were set at 10 and 50 Hz, respectively, the SNR for the two hydrophone-measured signals, were found to be –6.7 and 2.7 dB at positions 1 and 2, respectively.

The effect of the low-pass filter cut-off frequency on the cross-correlation coefficient is demonstrated in Fig. 6. The filter cut-off frequencies were set at 10 Hz for the high-pass filter, and the cut-off frequencies ranged from 30 to 200 Hz for the low-pass filters.

In the theoretical model, the cross-correlation coefficient is mainly determined by the lower cut-off frequency, provided that the bandwidth of the leak noise is relatively broad. This effect can be seen by comparing Figs. 6(d), (f) with (h), which are very similar. In contrast, a slight difference can be seen in Fig. 6(b) because in this case the theoretical correlation coefficient is governed by both the lower and upper cut-off frequencies as the bandwidth is small. A similar trend can be seen in the experimental results plotted in Figs. 6(a) and (c), where there is a slight difference in the correlation coefficients when the low-pass filters are set at 30 and 50 Hz. Furthermore, when the low-pass filter cut-off frequencies are adjusted to values above 50 Hz, the correlation coefficients do not change as shown in Figs. 6(e) and (g). This indicates that most information about the leak signal is concentrated below 50 Hz, which can also be seen in Fig. 5, which shows that the ambient noise measured by the hydrophones dominates above 50 Hz. Thus for hydrophone-measured signals in this case, the low-pass filter cut-off frequency can be set at 50 Hz.

Fig. 7 shows the effect of the high-pass filter cut-off frequency for both experimental results and predictions. As before, theoretical predictions of the cross-correlation coefficients are adjusted to account for the presence of background noise. The cut-off frequencies of the low-pass filters are 50 Hz and those of the high-pass filters from 5 to 40 Hz.

For the correlation coefficients derived from the hydrophone-measured signals as shown in Figs. 7(c), (e) and (g), a definite peak is obtained despite the narrow frequency band of the leak signal. The oscillatory behaviour of the correlation function becomes more obvious as the pass band of the leak signal becomes smaller. The time delay is estimated to be in the range 0.090–0.094 s and the position of the leak relative to point 1 is calculated to be 72.9–73.8 m. However, three anomalous peaks can be seen in Fig. 7(a), which are caused by the interference of low frequency background noise at low frequencies below 10 Hz and may present false time delay estimators. In addition, a definite peak cannot always be obtained when the cut-off frequency of

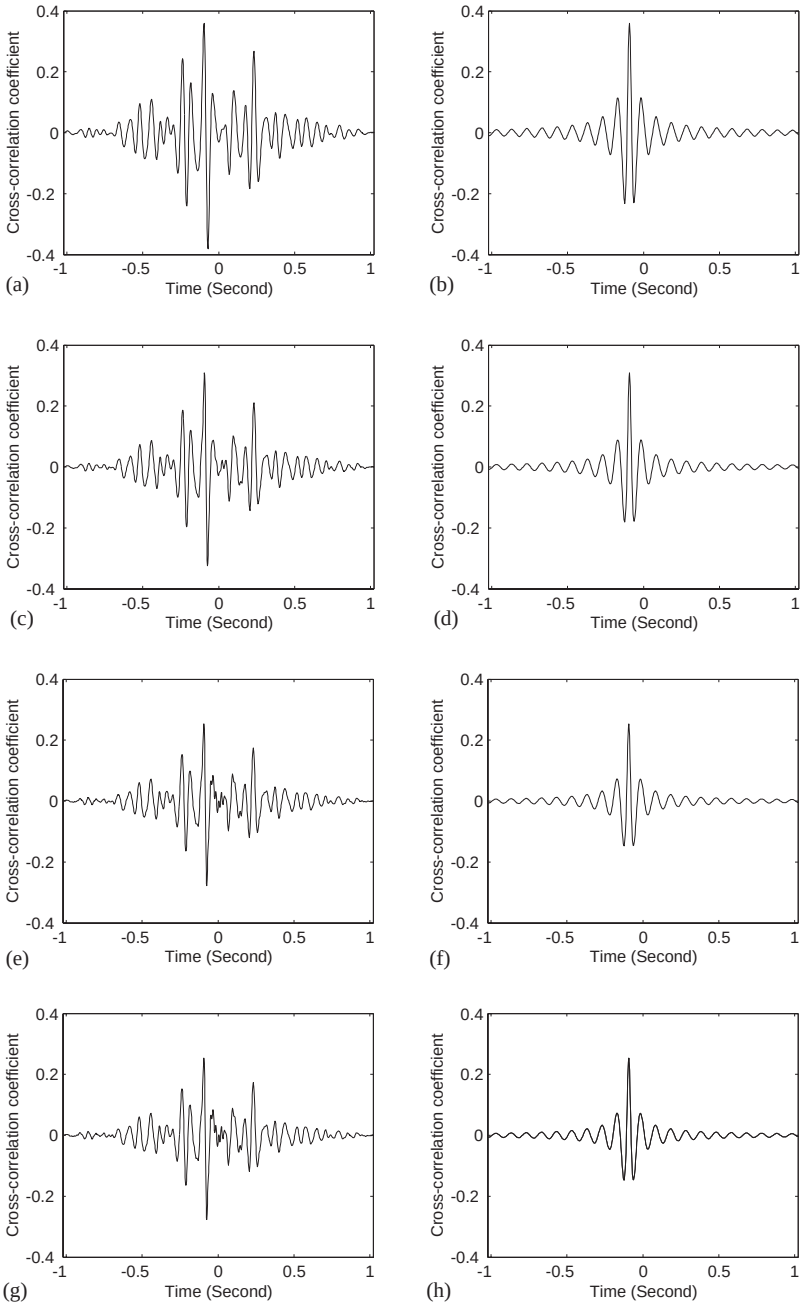

Fig. 6. Effect of the low-pass filter cut-off frequency on the cross-correlation coefficient. The cut-off frequencies of the high-pass filters are set at 10 Hz. The low-pass filter cut-off frequencies are: (a) 30 Hz; (c) 50 Hz; (e) 100 Hz; (g) 200 Hz. Comparison of the corresponding theoretical values is made when the low-pass filter cut-off frequencies are set at: (b) 30 Hz; (d) 50 Hz; (f) 100 Hz; (h) 200 Hz.

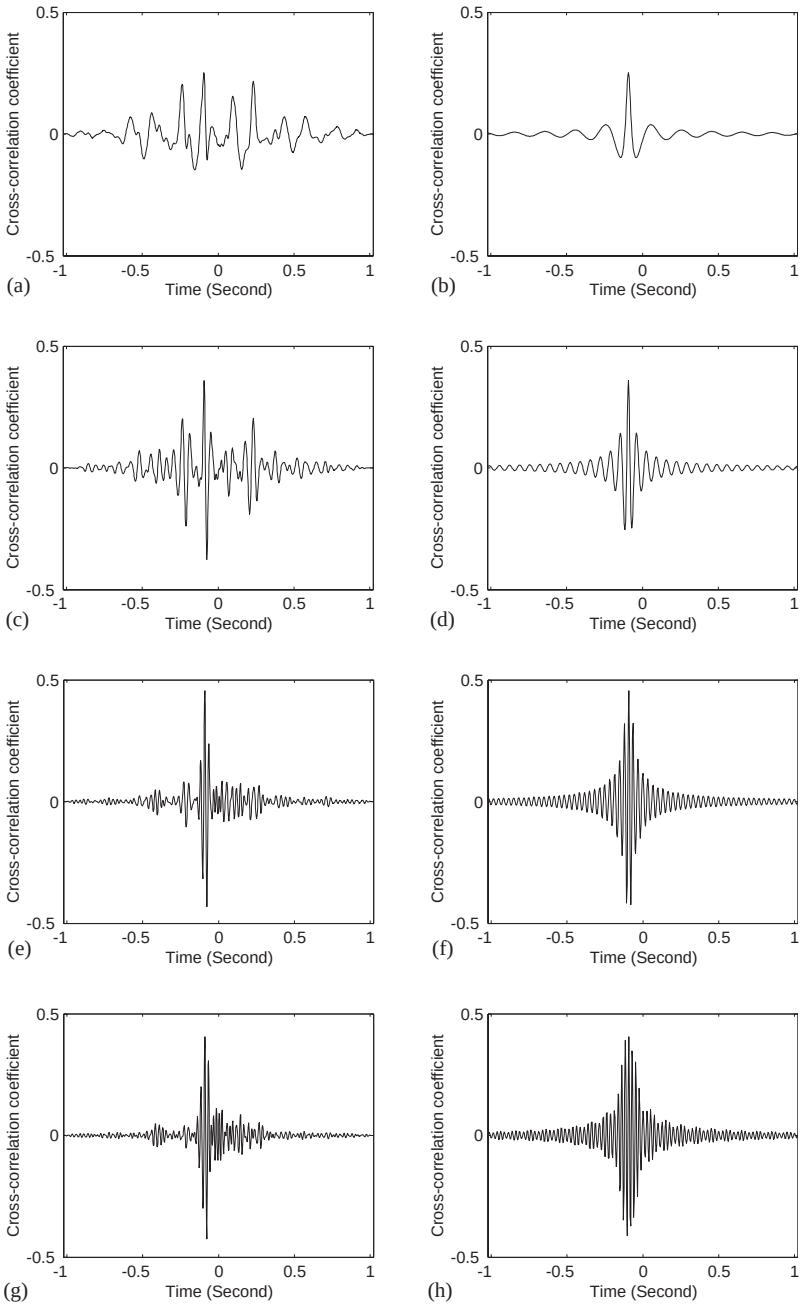

Fig. 7. Effect of the high-pass filter cut-off frequency on the cross-correlation coefficient. The cut-off frequencies of the low-pass filters are set at 50 Hz. The high-pass filter cut-off frequencies are: (a) 5 Hz; (b) 15 Hz; (c) 30 Hz; (d) 40 Hz. Comparison of the corresponding theoretical values is made when the high-pass filter cut-off frequencies are set at: (b) 5 Hz; (d) 15 Hz; (f) 30 Hz; (h) 40 Hz.

the high-pass filter is set below 10 Hz, as expected. Thus the high-pass filter cut-off frequency can be set at 10 Hz.

The corresponding theoretical values of the cross-correlation coefficients are plotted in Figs. 7(b), (d), (f) and (h). These graphs illustrate the same oscillatory behaviour of the correlation coefficients to that of the experimental results. The differences between the predictions and the experimental results are due to the effect of the background noise on the measured signals.

7. Conclusions

An analytical model of the cross-correlation function for wave propagation in buried plastic water pipes has been established, by combining the correlation technique with wave propagation theory in plastic pipes. This model has been applied to explain some of the main features of experimental data, including wave propagation and attenuation.

The model explains the importance of the cut-off frequency of the high-pass filter and the insensitivity of the correlation to the cut-off frequency of the low-pass filter to measurements of the cross-correlation. It has been shown that in the noise-free case, good levels of correlation are only possible for ratios of sensor distances from the leak of less than about 10 (or greater than 0.1). In practical situations, the achievement of good levels of correlation coefficients is further restricted because of undesirable correlated background noise.

The effect of the background noise on the model of the correlation has been presented. It has been shown that an estimate of the SNR at a measurement position can be simply determined from the ratio of the peak values of the experimental result of the correlation coefficient and its corresponding theoretical prediction.

Acknowledgements

The authors gratefully acknowledge the support of the EPSRC under grant GR/R13937/01 and discussions with Roger Ironmonger of Primayer Ltd.

References

[1] M. Fantozzi, G.D. Chirico, E. Fontana, F. Tonolini, Leak inspection on water pipelines by acoustic emission with cross-correlation method, *Annual Conference Proceeding, American Water Works Association, Engineering and Operations*, San Antonio, Texas, 1993, pp. 609–621.

[2] H.V. Fuchs, R. Riehle, Ten years of experience with leak detection by acoustic signal analysis, *Applied Acoustics* 33 (1991) 1–19.

[3] D.A. Liston, J.D. Liston, Leak detection techniques, *Journal of the New England Water Works Association* 106 (1992) 103–108.

[4] G.J. Weil, Non contact, remote sensing of buried water pipeline leaks using infrared thermography, Water Resources Planning and Management and Urban Water Resources, 1993, pp. 404–407.

[5] R.S. Pudar, J.A. Liggett, Leaks in pipe networks, *Journal of Hydraulic Engineering, American Society of Civil Engineers* 118 (1992) 1031–1046.

[6] K.W. Sneddon, G.R. Olhoeft, M.H. Powers, Determining and mapping DNAPL saturation values from noninvasive GPR measurements, *Symposium on the Application of Geophysics to Environmental and Engineering Problems*, Arlington, Virginia, 2000, pp. 293–302.
[7] O. Hunaidi, Ground-penetrating radar for detection of leaks in buried plastic water distribution pipes, *Seventh International Conference on Ground-Penetrating Radar*, Lawrence, Kansas, 1998, pp. 783–786.
[8] O. Hunaidi, W. Chu, A. Wang, W. Guan, Detecting leaks in plastic pipes, *Journal of the American Water Works Association* 92 (2000) 82–94.
[9] O. Hunaidi, W.T. Chu, Acoustical characteristics of leak signals in plastic water distribution pipes, *Applied Acoustics* 58 (1999) 235–254.
[10] A.V. Oppenheim, R.W. Schafer, *Digital Signal Processing*, Prentice-Hall, Englewood Cliffs, NJ, 1975.
[11] C.R. Fuller, F.G. Fahy, Characteristics of wave propagation and energy distributions in cylindrical elastic shells filled with fluid, *Journal of Sound and Vibration* 81 (1982) 501–518.
[12] C.R. Fuller, The input mobility of an infinite circular cylindrical elastic shell filled with fluid, *Journal of Sound and Vibration* 87 (1983) 409–427.
[13] R.J. Pinnington, A.R. Briscoe, Externally applied sensor for axisymmetric waves in a fluid filled pipe, *Journal of Sound and Vibration* 173 (1994) 503–516.
[14] J.M. Muggleton, M.J. Brennan, R.J. Pinnington, Development of a water pipe monitoring system for leak detection: experimental work, Technical Memorandum 860, ISVR, Southampton, 2001.
[15] J.M. Muggleton, M.J. Brennan, R.J. Pinnington, Wavenumber prediction of waves in buried pipes for water leak detection, *Journal of Sound and Vibration* 249 (2002) 934–954.